Hindawi Publishing Corporation
Journal of Nanomaterials
Volume 2014, Article ID 164380, 8 pages
http://dx.doi.org/10.1155/2014/164380

Research Article

Low-Temperature Synthesis and Gas Sensitivity of Perovskite-Type $LaCoO_3$ Nanoparticles

Lorenzo Gildo Ortiz,[1] Héctor Guillén Bonilla,[1] Jaime Santoyo Salazar,[2] M. de la L. Olvera,[3] T. V. K. Karthik,[3] Enrique Campos González,[2] and Juan Reyes Gómez[4]

[1] *Facultad de Ciencias Químicas, Universidad de Colima, 28400 Colima, COL, Mexico*
[2] *Departamento de Física, Centro de Investigación y de Estudios Avanzados del Instituto Politécnico Nacional, 07360 México, DF, Mexico*
[3] *Departamento de Ingeniería Eléctrica-SEES, Centro de Investigación y de Estudios Avanzados del Instituto Politécnico Nacional, 07360 México, DF, Mexico*
[4] *Facultad de Ciencias, Universidad de Colima, Bernal Díaz del Castillo 340, 28045 Colima, COL, Mexico*

Correspondence should be addressed to Juan Reyes Gómez; reyesgj@ucol.mx

Received 29 January 2014; Revised 31 March 2014; Accepted 16 May 2014; Published 5 June 2014

Academic Editor: Rakesh K. Joshi

$LaCoO_3$ nanoparticles with perovskite-type structure were prepared by a microwave-assisted colloidal method. Lanthanum nitrate, cobalt nitrate, and ethylenediamine were used as precursors and ethyl alcohol as solvent. The thermal decomposition of the precursors leads to the formation of $LaCoO_3$ from a temperature of 500°C. The structural, morphological, and compositional properties of $LaCoO_3$ nanoparticles were studied in this work by X-ray diffraction (XRD), scanning electron microscopy (SEM), transmission electron microscopy (TEM), and atomic force microscopy (AFM). Pellets were manufactured in order to test the gas sensing properties of $LaCoO_3$ powders in carbon monoxide (CO) and propane (C_3H_8) atmospheres. Agglomerates of nanoparticles with high connectivity, forming a porous structure, were observed from SEM and TEM analysis. $LaCoO_3$ pellets presented a high sensitivity in both CO and C_3H_8 at different concentrations and operating temperatures. As was expected, sensitivity increased with the gas concentration and operation temperature increase.

1. Introduction

In the last years, inorganic materials have been widely studied due to their attractive characteristics, such as capacity to modify its microstructure, morphology, and other physical properties as a function of the method and conditions of synthesis [1–3]. Novelty synthesis methods have been developed for preparing inorganic materials, such as aerosol, sol-gel, solution, coprecipitation, solution-polymerization, colloidal method, and solid-state reaction (ceramic method), among others [4–10]. It is well known that a particular synthesis route induces to physical changes in the volume and surface characteristics of the material, for example, structure, morphology, porosity, and particle size [11], and consequently the electrical, optical, magnetic, and sensing properties are modified as well [12, 13].

In particular, diverse research groups have focused their interest in performing synthesis of materials through colloidal routes, since this method has led to process materials with particle size around a few nanometers, with attractive morphologies of a great relevance due to its potential applications [14, 15]. For example, Michel et al. obtained porous microspheres by using colloidal synthesis of trirutile-type $CoSb_2O_6$ [16]. Sun et al. also reported the formation of nanostructured microspheres of organic-inorganic hybrid materials by using the colloidal methods [17]. Nanoparticles synthesized by colloidal routes that can be applied in different fields, such as pigments for diverse applications, recording materials, ceramics, catalysis, drug delivery systems, biosensors, photonic crystals, colloidal lithography, porous membranes, and formation of hollow spheres, among others [17–19].

On the other hand, lanthanum cobalt oxide ($LaCoO_3$) with perovskite-type structure has acquired great importance by its magnetic, electrical, and catalytic properties that make it attractive for different technological applications. For example, it has been reported that $LaCoO_3$ exhibits catalytic activity in the oxidation of different compounds, like carbon monoxide (CO) and methane (CH_4), and also exhibits photocatalytic activity in the oxidation of methyl orange and water [20–27]. In addition, the $LaCoO_3$ is a material that presents good thermoelectric properties [28].

In this work, $LaCoO_3$ nanoparticles were synthesized by a colloidal route for studying their physical properties. Additionally, the synthesized $LaCoO_3$ powders were used to manufacture pellets to be tested as gas sensors in two different atmospheres, namely, CO and propane (C_3H_8).

2. Experimental Procedures

2.1. Synthesis of $LaCoO_3$ Nanoparticles. $LaCoO_3$ nanoparticles with perovskite-type structure were prepared employing a colloidal method. Firstly, three different solutions were separately prepared. The first one consisted of 1.7316 g of $La(NO_3)_3{\cdot}6H_2O$ (Alfa Aesar), the second 1.164 g of $Co(NO_3)_2{\cdot}6H_2O$ (Jalmek), both dissolved in 5 mL of absolute ethyl alcohol (CTR), and the third 2 mL of ethylenediamine (Sigma) dissolved in 10 mL of the same alcohol. The three solutions were stirred vigorously for 20 min and then mixed all together. Finally, the resultant solution was kept in stirring for 24 h at room temperature.

Later, the solution was put into a domestic microwave oven (LG model, MS1147 X) in order to evaporate the solvent by a low power radiation of microwaves (~145 W). The evaporation rate was controlled by applying the microwave radiation in steps of 25 s in order to keep the solution at a temperature around 70°C; the temperature was monitored by an Extech IR 403255 thermometer. The control of heating time and temperature was decisive to avoid the splashing and the consequent loss of material, namely, a better process yield. After entire evaporation of solvents a yellow paste was obtained, which was dried at 200°C during 8 h in a normal atmosphere. The resultant powder was divided in five parts, and they were calcined at different temperatures, namely, 300, 400, 500, 600, and 700°C. The calcination process consisted of a heating rate of 100°C/h, up to reach the set point, and then an annealing for 5 h at constant temperature. The calcinations were carried out in an oven Vulcan 3–550, which has a programmable temperature controller.

2.2. Physical Characterization of $LaCoO_3$ Powders. All calcined powders were analyzed by X-ray diffraction (XRD) by using a Siemens D500 diffractometer with a Cu-Kα radiation. The 2θ scanning range was from 10° to 70° with a step size of 0.02° and a step time of 1 s. Lattice parameters were calculated from the XRD patterns. Powder Cell 2.4 software [29] was employed for analyzing the XRD spectra. Morphology of $LaCoO_3$ powders was analyzed by scanning electron microscopy (SEM) by using a JEOL JSM-6390LV microscope in modality of high vacuum and secondary electron emission. A surface composition analysis was developed by energy dispersive X-ray spectroscopy (EDS-SEM) with an XFlash Detector 5010 from Bruker. Surface area analysis was performed by nitrogen adsorption at 77 K, with a Minisorp II equipment from BEL Japan. In this characterization, previous to the N_2 adsorption process, the chamber with the sample was outgassed and kept in vacuum for 24 h, at room temperature. Surface area was calculated from the BET equation. Size and shape of the nanoparticles were analyzed by transmission electron microscopy (TEM) in a JEM-2010 equipment from JEOL, with an acceleration voltage of 200 kV. The surface topography was analyzed by atomic force microscopy (AFM) by using a JSPM-5200 microscope from JEOL under intermittent contact operation. For the topographical study, 0.1 g of $LaCoO_3$ powder was dispersed with isopropyl alcohol in a container, by using an ultrasonic bath for 5 minutes. Later, by a syringe, a drop of material disperse was deposited over the surface of a 15 mm diameter bronze disc and finally dried at room temperature during 24 h.

2.3. Pellets Preparation for Gas Sensitivity Analysis. The sensing properties of synthesized $LaCoO_3$ powders were probed in two different atmospheres, namely, carbon monoxide (CO) and propane (C_3H_8), at different gas concentrations and operation temperatures. The sensing measurements consisted of monitoring the electrical resistance of 12 mm diameter and 0.5 mm thick pellets, manufactured by using a Simplex Ital Equip-25 Tons pressing machine. After several trials, optimal pressing conditions were found for 15 tons during 90 min. For electrical measurements two ohmic contacts were manufactured onto the pellets by using pure silver paint (Alpha Aesar). Then, these pellets were put onto a sample holder in a chamber, which allows the introduction of gases in a controlled way. For controlling gas concentration, the partial pressure into the chamber was monitored by a TM20 Leybold detector. The experimental setup used for measuring the sensing response is shown in Figure 1.

The pellets sensitivity, S, was estimated by the relative difference of the electrical conductances (1/electrical resistance), according to the following equation:

$$S = \frac{G_g - G_o}{G_o}, \tag{1}$$

where G_g and G_o are the electrical conductance of the $LaCoO_3$ pellets measured in gas (CO or C_3H_8) and air, respectively. The conductance was measured by using a Keithley 2001 digital multimeter as a function of operating temperature and gas concentration. Corresponding graphs are reporting results for three temperatures, namely, 150, 250, and 350°C, and five different gas concentrations, 5, 50, 100, 200, and 300 ppm. This temperature range was selected since lower operating temperatures do not lead to any conductance changes.

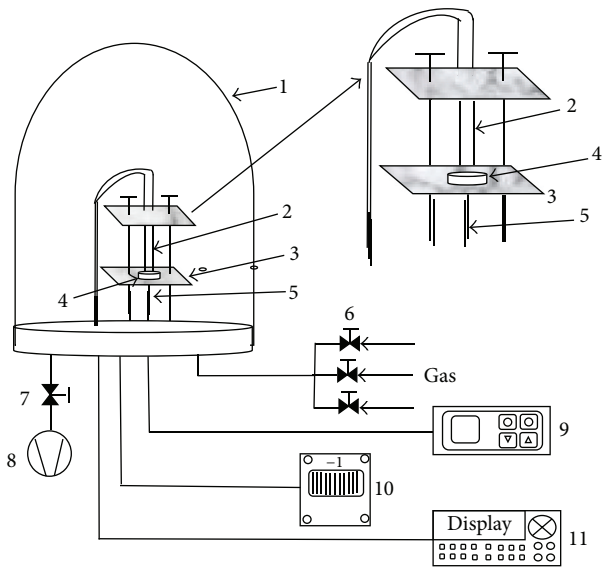

(1) Vacuum chamber
(2) Probes
(3) Heating resistance plate
(4) Sample
(5) Thermocouple
(6) Gas valves
(7) Vacuum valve
(8) Pumping system
(9) Temperature controller
(10) Pressure meter
(11) Multimeter

Figure 1: Schematic diagram of the system used for monitoring the sensing properties in controlled atmosphere and temperature.

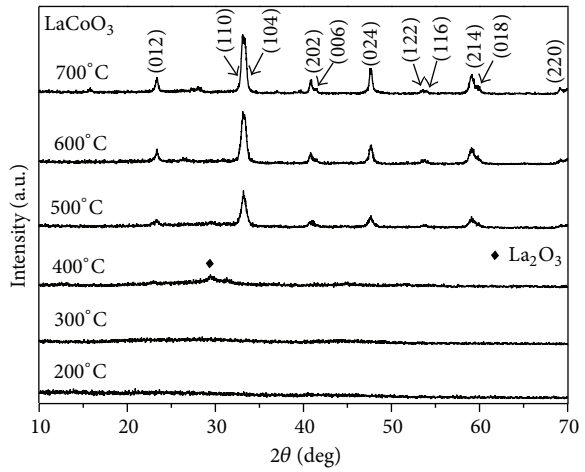

Figure 2: XRD patterns of the precursor material calcined from 200 to 700°C.

3. Results and Discussion

3.1. XRD Analysis. Figure 2 shows the X-ray diffraction patterns of the $LaCoO_3$ powders obtained after thermal treatments carried out from 200 to 700°C. From the spectra array it can be observed that powders calcined at 200 and 300°C are totally amorphous, since the corresponding diffraction patterns do not show defined peaks. The spectrum of powders calcined at 400°C shows a weak peak corresponding to the La_2O_3 phase according to the JCPDS file number 05-0602, whereas the spectrum of powders calcined at 500°C fit well to the crystalline structure of $LaCoO_3$ with the presence of the (012), (110), (104), (202), (006), (024), (122), (116), (214), (018), and (220) planes, according to the JCPDF file number 48-0123 card. At higher calcination temperatures, 600 and 700°C, the peaks in the spectra are higher and better defined. This result is associated with a better crystallinity. These two spectra prove the formation of the $LaCoO_3$ perovskite with rhombohedral structure with space group R-3c. The symmetry is consistent with other XRD studies reported previously [28, 30]. The lattice parameters estimated were a = 5.434 Å and c = 13.110 Å. The wide peaks in the diffraction spectra indicate the nanocrystalline nature of the material; therefore, the mean size of crystal (t) was estimated by using the Scherrer equation [31], $t = 0.9\lambda/\beta\cos\theta$, where λ is the wavelength of the radiation used (1.5406 Å), θ is the Bragg angle, and β is the full width at half maximum (FWHM) of the diffraction peak. Considering all reflections, the crystal size estimated was around 30 nm.

Traditionally, $LaCoO_3$ has been synthesized through a solid-state reaction, employing La_2O_3 as precursor material, whereas Co_2O_3 or Co_3O_4 were required to mix, press, and calcinate the solid precursors at temperatures as high as 1000°C and long times for reactions (in the order of days) for having a complete formation of the compound [28, 32]. Comparing the solid-state reaction with the synthesis by colloidal method, the formation temperatures of 600 and 700°C and the annealing time of 5 h are relatively low for the formation of $LaCoO_3$.

Recently, other research groups have reported different methods for preparing $LaCoO_3$, where calcination temperatures between 600 and 700°C were used. Carabalí et al. [33] synthesized $LaCoO_3$ by the acrylamide polymerization method using γ radiation, reporting that the compound begins its formation at 500°C and the formation of the single phase was around 700°C. Jung and Hong [24] reported the formation of $LaCoO_3$ at 650°C when it was prepared from an aqueous solution of metallic nitrate salts in presence of malic acid, later a drying process by microwave radiation, and finally a thermal treatment. Similarly, Sompech et al. [34] synthesized perovskite at 600°C employing a mechanochemical method. In the present work, $LaCoO_3$ powders were obtained employing a microwave-assisted colloidal method in presence of ethylenediamine and a further calcination process from a temperature of 500°C and higher. Then, we can state that temperatures around 600°C are suitable for the formation of $LaCoO_3$ employing soft synthesis methods.

3.2. Scanning Electron Microscopy Analysis. Figure 3 shows two typical SEM images of $LaCoO_3$ powders after calcination at 700°C. These images present two different magnifications: (a) 500x and (b) 15000x. In Figure 3(a) it can be observed that the surface presents lots of pores with different sizes, around a few micrometers. The smallest pores are around 0.5 μm, whereas the biggest are around 30 μm. Also a grid of particles was observed forming net-like structures and some particles disperse over the surface of material. This can be more clearly observed at higher magnifications; as is shown in Figure 3(b)

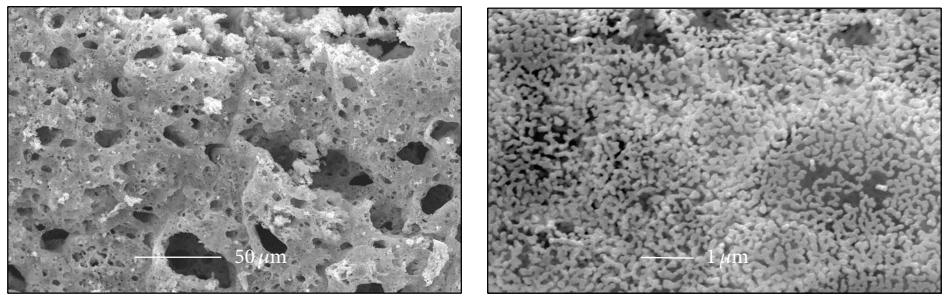

(a) (b)

Figure 3: SEM images of $LaCoO_3$ powders calcined at 700°C at two different magnifications: (a) 500x and (b) 15000x.

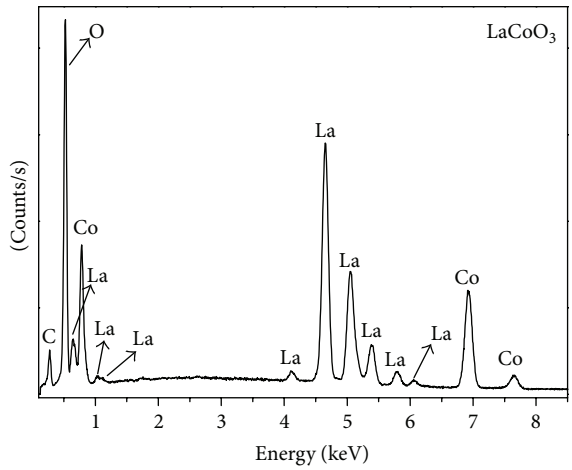

Figure 4: EDS-SEM spectrum of $LaCoO_3$ powders showing characteristic lines of La, Co, and O.

the gridding is due to the great connectivity among the particles. The porous microstructure obtained is attributed to the released gases during the thermal decomposition of the organic species, mainly water vapor, NO_x, and CO_2, among others [35]. BET surface area of $LaCoO_3$ was around 14.2 m^2/g.

The preparation of inorganic compounds employing colloidal methods has been widely studied by Matijevic [36]. The author states that these methods give rise to a better control on the nucleation process and the growth of the particles. Thus, compounds with different morphologies can be obtained. These morphologies follow the crystallization principles given by Lamer and Dinegar [37], which were described in three theoretical stages; the first stage states that the concentration of the reagents in colloidal dispersions gradually increases, the second one states that the concentration of the reagents reaches a limiting state of supersaturation and the nucleation happens forming the nuclei of the crystals, and finally the third stage states that the growth of stable nuclei to form discrete particles is originated by diffusion of the dissolved species to nuclei.

Figure 4 shows an EDS-SEM spectrum of $LaCoO_3$ oxide. From this, it is possible to observe the characteristic peaks of La, Co, and O in concordance to the chemical composition of the material. For lanthanum (La), more intensive peaks correspond to the Lα and Lβ lines, localized at 4.65 and 5.04 keV, respectively. For cobalt (Co), the three peaks present in the spectrum correspond to the characteristic lines Lα, Kα, and K$_\beta$, localized at 0.77, 6.92, and 7.65 keV, respectively. Finally, for oxygen (O), the corresponding line is Kα, with an energy value of 0.525 keV. On the other hand, the line localized close to 0.28 keV indicates that carbon (C) element is present in the composition, which is a residue of the combustion of the organic material [38]. This fact is a disadvantage of employing the organic reagents in the synthesis of inorganic compounds.

3.3. Transmission Electron Microscopy Analysis. Figure 5 shows typical images obtained by transmission electron microscopy and their corresponding particle size distribution of $LaCoO_3$ perovskite powders. In Figure 5(a) we observed that $LaCoO_3$ oxide is constituted by nanoparticles that present irregular shape and a rough surface texture. In addition, a continuous connectivity among the particles was observed as well, in a similar way to that observed in the SEM image Figure 3(b). This micrograph evidences the formation of necks for giving rise, one more time, to the coalescence of particles. Figure 5(b) shows the particle size distribution of $LaCoO_3$ oxide obtained through the analysis of various TEM images. The particle size has been estimated in a range of 25 to 144 nm, and around 78% of the particles were in the 40–100 nm range, with an average size estimated around 68 nm, with a standard deviation of 27 nm. HRTEM was performed in a selected zone of the sample. The HRTEM image reveals that the interplanar distance is around 3.86 Å, which corresponds to (012) planes. This image reports the electron diffraction pattern, where the characteristic rings of the reflections of the nanometric polycrystalline material can be observed.

3.4. Atomic Force Microscopy Analysis. Topography of the $LaCoO_3$ powders was analyzed by using the atomic force microscopy (AFM) technique. Figure 6 shows a typical AFM image in a 322 nm × 322 nm scanned area. From this micrograph, a topography can be observed that is conformed by grains of different height, associated directly with the contrast of the image. The estimated particle size of the scanned area was around 64 nm. These results are consistent

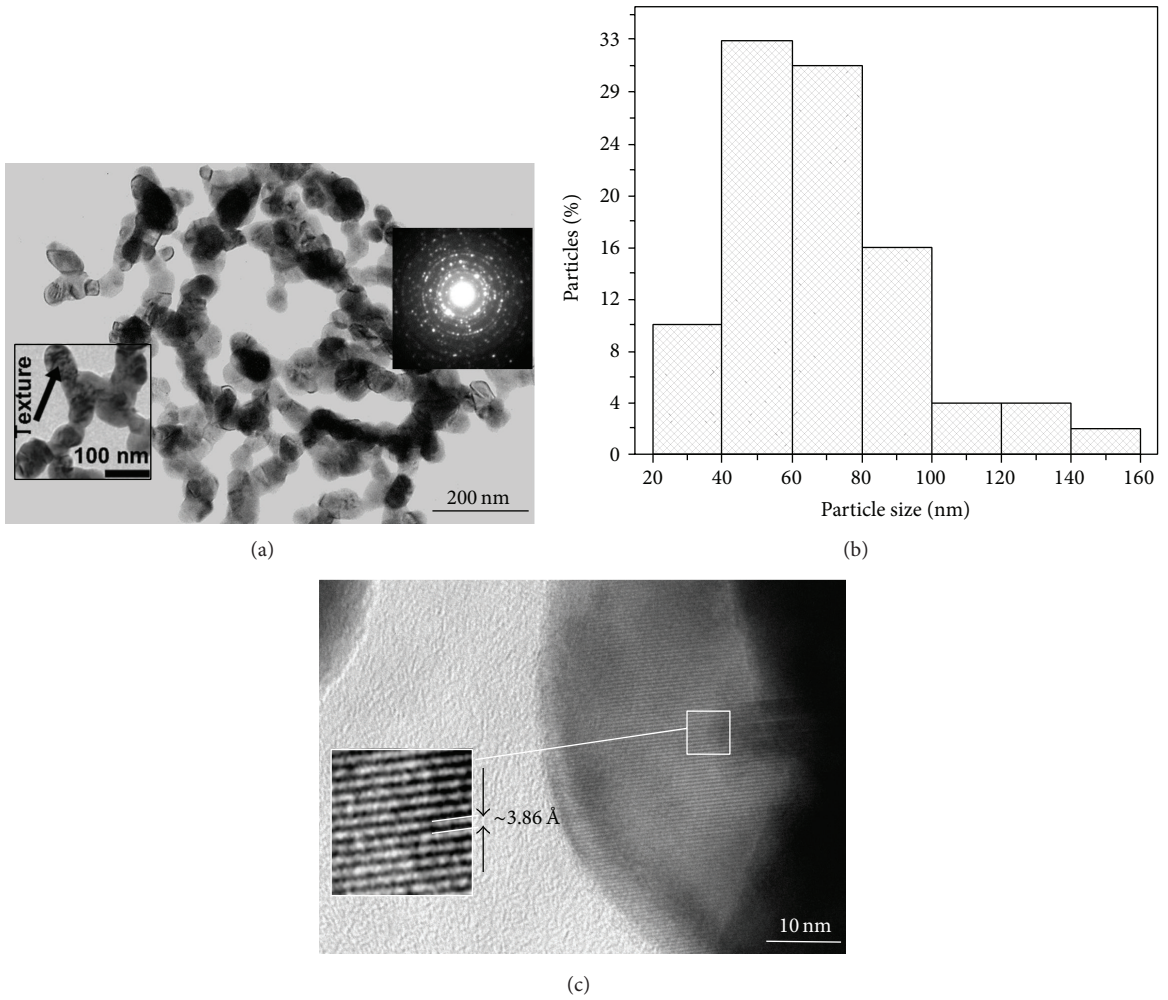

FIGURE 5: TEM analysis of $LaCoO_3$ powders: (a) $LaCoO_3$ nanoparticles and electron diffraction pattern (inset), (b) particle size distribution, and (c) HRTEM image showing the lattice fringes.

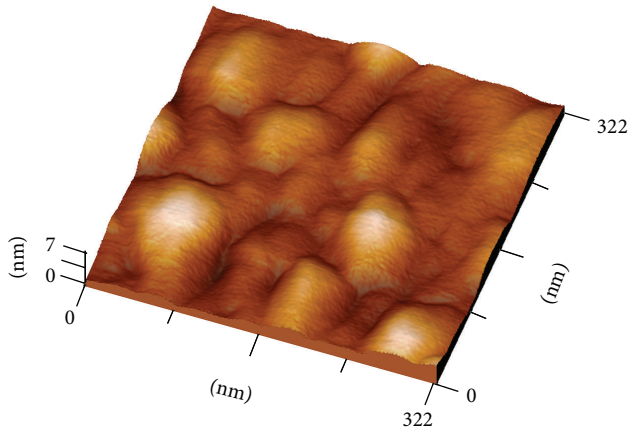

FIGURE 6: Topographical image obtained by AFM of $LaCoO_3$ powders.

with those obtained from TEM, shown in Figure 5(a). The mean planar roughness estimated over the scanning area was around 4.84 nm. From AFM analysis it is evident that the texture observed from TEM images can be associated to the roughness on the nanoparticles surface.

3.5. Sensing Properties. Figure 7 shows the sensitivities of the $LaCoO_3$ pellets as a function of the CO and C_3H_8 concentration. $LaCoO_3$ pellets are clearly sensible to both gas concentration and operating temperature; nevertheless, at temperatures below 150°C no resistance changes were registered. We observed an increase in the sensitivity magnitude with increase in the operation temperature for both CO and C_3H_8. This result is associated to the increase of the oxygen desorption at higher temperatures. Chang reported the adsorption of different oxygen species as a function of the temperature [39]. So, at temperature below 150°C the O_2^- oxygen species is present in a dominant way, whereas other oxygen species, like O^- and O^{2-}, are present at higher temperatures, which are more reactive species than previous ones. At room temperature no resistance changes are registered, since there is not enough thermal energy to produce the desorption of oxygen species, irrespective of the gas concentration.

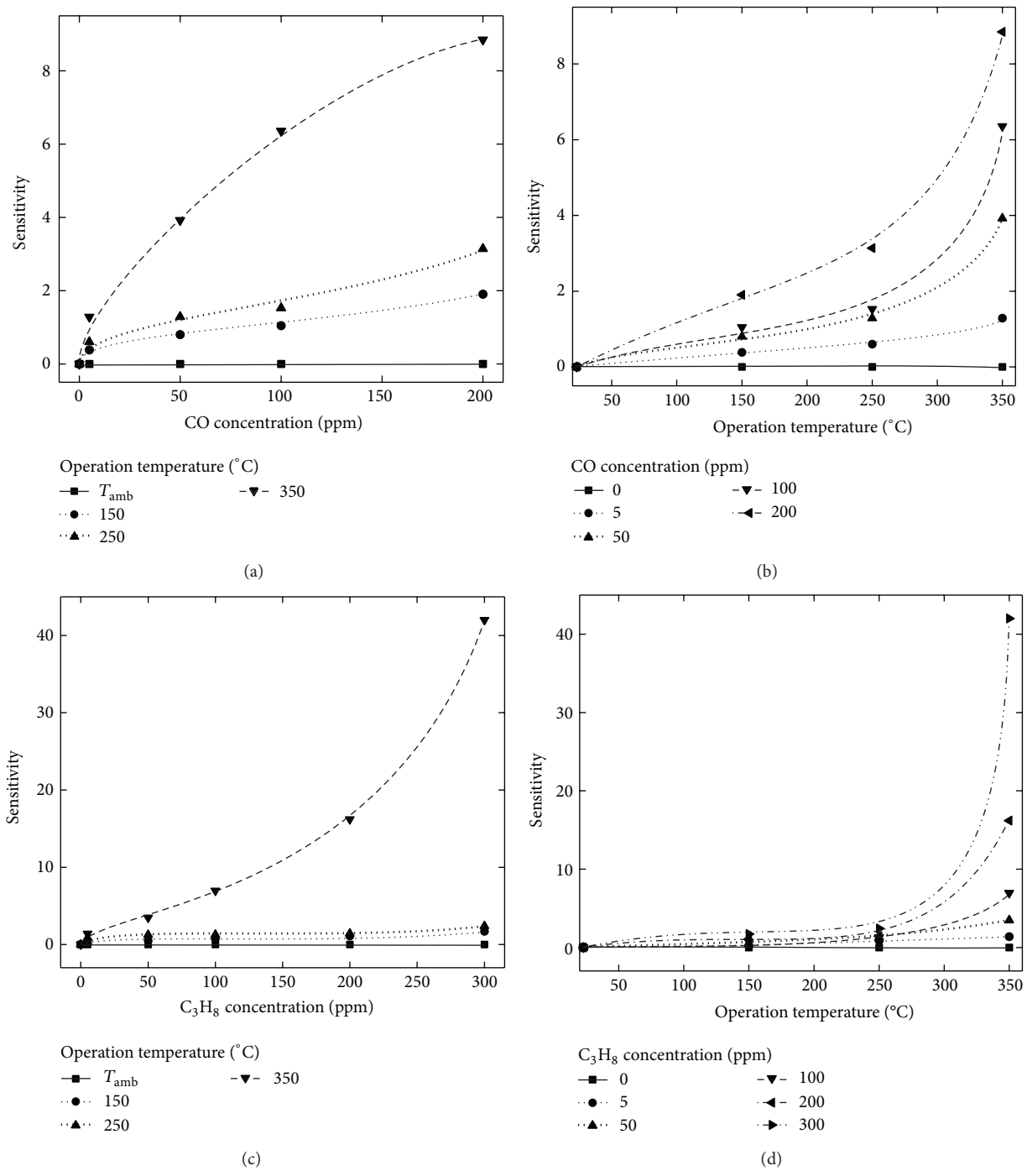

FIGURE 7: Sensitivity of $LaCoO_3$ pellets versus (a) CO concentration, (b) operating temperature and CO, (c) propane (C_3H_8) concentration, and (d) operating temperature and propane (C_3H_8) concentration.

At 350°C and 200 ppm of CO and C_3H_8, the sensitivities calculated were around 10 and 15, respectively. Nevertheless, in case of C_3H_8, the sensitivity was around 42, at 300 ppm; thus, it was thrice increased. On the other hand, the sensitivity was increased with the gas concentration, irrespective of the gas type, as was expected, since the more gas concentration the more desorption reactions.

4. Conclusions

$LaCoO_3$ nanoparticles with perovskite-type structure were successfully synthesized employing a colloidal method. This synthesis route is a convenient way to synthesize the compound at temperatures relatively low. $LaCoO_3$ nanoparticles are clearly sensible to both operating temperature and gas

concentration. As was expected, sensitivity of $LaCoO_3$ pellets increased by increasing the CO and C_3H_8 concentration and the operation temperature. Maximum sensitivity, around 42, was obtained in C_3H_8 at 350°C for a concentration of 300 ppm.

Conflict of Interests

The authors declare that there is no conflict of interests regarding the publication of this paper.

Acknowledgments

Lorenzo Gildo Ortiz and Héctor Guillén Bonilla express their gratitude to Consejo Nacional de Ciencia y Tecnología (CONACyT) for the scholarships received. The technical assistance of Darío Pozas Zepeda and Miguel Ángel Luna Arias is thanked. This work was partially supported by Project no. 784-12 FRABA, and Project no. 155996 from CONACyT, managed by M. de la L. Olvera.

References

[1] R. Betancourt-Galindo, P. Y. Reyes-Rodriguez, B. A. Puente Urbina et al., "Synthesis of copper nanoparticles by thermal decomposition and their antimicrobial properties," *Journal of Nanomaterials*, vol. 2014, Article ID 980545, 5 pages, 2014.

[2] S. Wannapop, T. Thongtem, and S. Thongtem, "Characterization of donut-like $SrMoO_4$ produced by microwave-hydrothermal process," *Journal of Nanomaterials*, vol. 2013, Article ID 474576, 6 pages, 2013.

[3] A. Phuruangrat, T. Thongtem, and S. Thongtem, "Influence of PVP on the morphologies of BiS_3 nanostructures synthesized by solvothermal method," *Journal of Nanomaterials*, vol. 2013, Article ID 314012, 6 pages, 2013.

[4] J. Ortega, T. T. Kodas, S. Chadda, D. M. Smith, M. Ciftcioglu, and J. E. Brennan, "Formation of dense $Ba_{0.86}Ca_{0.14}TiO_3$ particles by aerosol decomposition," *Chemistry of Materials*, vol. 3, no. 4, pp. 746–751, 1991.

[5] J. D. Jordan, R. A. Dunbar, D. J. Hook et al., "Production, characterization, and utilization of aerosol-deposited sol-gel-derived films," *Chemistry of Materials*, vol. 10, no. 4, pp. 1041–1051, 1998.

[6] C. R. Michel, E. Delgado, G. Santillán, A. H. Martínez, and A. Chávez-Chávez, "An alternative gas sensor material: synthesis and electrical characterization of $SmCoO_3$," *Materials Research Bulletin*, vol. 42, pp. 84–93, 2007.

[7] C. R. Michel, A. H. Martínez, and S. Jiménez, "Gas sensing response of nanostructured trirutile-type $CoSb_2O_6$ synthesized by solution-polymerization method," *Sensors and Actuators B*, vol. 132, no. 1, pp. 45–51, 2008.

[8] D. Wang and F. Caruso, "Polyelectrolyte-coated colloid spheres as templates for sol-gel reactions," *Chemistry of Materials*, vol. 14, no. 5, pp. 1909–1913, 2002.

[9] R. J. Hunter, *Foundations of Colloid Science*, Oxford University Press, New York, NY, USA, 2005.

[10] S. W. You, I. H. Kim, S. M. Choi, and W. S. Seo, "Solid-state synthesis and thermoelectric properties of $Mg_{2+x}Si_{0.7}Sn_{0.3}Sb_m$," *Journal of Nanomaterials*, vol. 2013, Article ID 815925, 4 pages, 2013.

[11] Y. Zhu, W. Zhao, H. Chen, and J. Shi, "A simple one-pot self-assembly route to nanoporous and monodispersed Fe_3O_4 particles with oriented attachment structure and magnetic property," *Journal of Physical Chemistry C*, vol. 111, no. 14, pp. 5281–5285, 2007.

[12] M. J. Molaei, A. Ataie, S. Raygan et al., "Magnetic property enhancement and characterization of nano-structured barium ferrite by mechano-thermal treatment," *Materials Characterization*, vol. 63, pp. 83–89, 2012.

[13] L. da Conceição, C. R. B. Silva, N. F. P. Ribeiro, and M. M. V. M. Souza, "Influence of the synthesis method on the porosity, microstructure and electrical properties of $La_{0.7}Sr_{0.3}MnO_3$ cathode materials," *Materials Characterization*, vol. 60, no. 12, pp. 1417–1423, 2009.

[14] S. Libert, D. V. Goia, and E. Matijević, "Internally composite uniform colloidal cadmium sulfide spheres," *Langmuir*, vol. 19, no. 26, pp. 10673–10678, 2003.

[15] S.-M. Yang, S.-H. Kim, J.-M. Lim, and G.-R. Yi, "Synthesis and assembly of structured colloidal particles," *Journal of Materials Chemistry*, vol. 18, no. 19, pp. 2177–2190, 2008.

[16] C. R. Michel, H. Guillén-Bonilla, A. H. Martínez-Preciado, and J. P. Morán-Lázaro, "Synthesis and gas sensing properties of nanostructured $CoSb_2O_6$ microspheres," *Sensors and Actuators B*, vol. 143, no. 1, pp. 278–285, 2009.

[17] X. Sun, S. Dong, and E. Wang, "Coordination-induced formation of submicrometer-scale, monodisperse, spherical colloids of organic-inorganic hybrid materials at room temperature," *Journal of the American Chemical Society*, vol. 127, no. 38, pp. 13102–13103, 2005.

[18] E. Matijević, "Preparation and properties of uniform size colloids," *Chemistry of Materials*, vol. 5, no. 4, pp. 412–426, 1993.

[19] M. G. Han and S. H. Foulger, "Crystalline colloidal arrays composed of poly(3,4-ethylenedioxythiophene)-coated polystyrene particles with a stop band in the visible regime," *Advanced Materials*, vol. 16, no. 3, pp. 231–234, 2004.

[20] F. Teng, S. Liang, B. Gaugeu, R. Zong, W. Yao, and Y. Zhu, "Carbon nanotubes-templated assembly of $LaCoO_3$ nanowires at low temperatures and its excellent catalytic properties for CO oxidation," *Catalysis Communications*, vol. 8, no. 11, pp. 1748–1754, 2007.

[21] B. Seyfi, M. Baghalha, and H. Kazemian, "Modified $LaCoO_3$ nano-perovskite catalysts for the environmental application of automotive CO oxidation," *Chemical Engineering Journal*, vol. 148, no. 2-3, pp. 306–311, 2009.

[22] A. Baiker, P. E. Marti, P. Keusch, E. Fritsch, and A. Reller, "Influence of the *A*-site cation in $ACoO_3$ (*A* = La, Pr, Nd, and Gd) perovskite-type oxides on catalytic activity for methane combustion," *Journal of Catalysis*, vol. 146, no. 1, pp. 268–276, 1994.

[23] Y. Wang, J. Ren, Y. Wang et al., "Nanocasted synthesis of mesoporous $LaCoO_3$ perovskite with extremely high surface area and excellent activity in methane combustion," *Journal of Physical Chemistry C*, vol. 112, no. 39, pp. 15293–15298, 2008.

[24] W. Y. Jung and S.-S. Hong, "Synthesis of $LaCoO_3$ nanoparticles by microwave process and their photocatalytic activity under visible light irradiation," *Journal of Industrial and Engineering Chemistry*, vol. 19, no. 1, pp. 157–160, 2013.

[25] Y. Yamada, K. Yano, D. Hong, and S. Fukuzumi, "$LaCoO_3$ acting as an efficient and robust catalyst for photocatalytic water oxidation with persulfate," *Physical Chemistry Chemical Physics*, vol. 14, no. 16, pp. 5753–5760, 2012.

[26] A. V. Salker, N.-J. Choi, J.-H. Kwak, B.-S. Joo, and D.-D. Lee, "Thick films of In, Bi and Pd metal oxides impregnated in $LaCoO_3$ perovskite as carbon monoxide sensor," *Sensors and Actuators B*, vol. 106, no. 1, pp. 461–467, 2005.

[27] M. Ghasdi and H. Alamdari, "CO sensitive nanocrystalline $LaCoO_3$ perovskite sensor prepared by high energy ball milling," *Sensors and Actuators B*, vol. 148, no. 2, pp. 478–485, 2010.

[28] L. Fu and J.-F. Li, "Preparation and thermoelectric properties of $LaCoO_3$ ceramics," *Key Engineering Materials*, vol. 434-435, pp. 404–408, 2010.

[29] W. Kraus and G. Nolze, *PowderCell For Windows. Version 2.4*, Federal Institute for Materials Research and Testing, Berlin, Germany, 2000.

[30] J. Prado-Gonjal, Á. M. Arévalo-López, and E. Morán, "Microwave-assisted synthesis: a fast and efficient route to produce $LaMO_3$ (M = Al, Cr, Mn, Fe, Co) perovskite materials," *Materials Research Bulletin*, vol. 46, no. 2, pp. 222–230, 2011.

[31] U. Holzwarth and N. Gibson, "The Scherrer equation versus the 'Debye-Scherrer equation'," *Nature Nanotechnology*, vol. 6, no. 9, p. 534, 2011.

[32] O. Myakush, V. Berezovets, A. Senyshyn, and L. Vasylechko, "Preparation and crystal structure of new perovskite-type cobaltites $R_{1-x}R'_xCoO_3$," *Chemistry of Metals and Alloys*, vol. 3, pp. 184–190, 2010.

[33] G. Carabalí, E. Chavira, I. Castro, E. Bucio, L. Huerta, and J. Jiménez-Mier, "Novel sol-gel methodology to produce $LaCoO_3$ by acrylamide polymerization assisted by γ-irradiation," *Radiation Physics and Chemistry*, vol. 81, no. 5, pp. 512–518, 2012.

[34] S. Sompech, A. Srion, and A. Nuntiya, "The effect of ultrasonic treatment on the particle size and specific surface area of $LaCoO_3$," *Procedia Engineering*, vol. 32, pp. 1012–1018, 2012.

[35] C. R. Michel, A. H. Martínez, F. Huerta-Villalpando, and J. P. Morán-Lázaro, "Carbon dioxide gas sensing behavior of nanostructured $GdCoO_3$ prepared by a solution-polymerization method," *Journal of Alloys and Compounds*, vol. 484, no. 1-2, pp. 605–611, 2009.

[36] E. Matijevic, "Uniform inorganic colloid dispersions. Achievements and challenges," *Langmuir*, vol. 10, no. 1, pp. 8–16, 1994.

[37] V. K. Lamer and R. H. Dinegar, "Theory, production and mechanism of formation of monodispersed hydrosols," *Journal of the American Chemical Society*, vol. 72, no. 11, pp. 4847–4854, 1950.

[38] V. V. Gorbunov, A. A. Shidlovskii, and L. F. Shmagin, "Combustion of transition-metal ethylenediamine nitrates," *Combustion, Explosion, and Shock Waves*, vol. 19, no. 2, pp. 172–173, 1983.

[39] S. C. Chang, "Oxygen chemisorption on tin oxide: correlation between electrical conductivity and EPR measurements," *Journal of Vacuum Science and Technology*, vol. 17, no. 1, pp. 366–369, 1979.